Biochimica et Biophysica Acta, 766 (1984) 513–524
Elsevier

BBA 41554

DISTRIBUTION OF LIGHT EXCITATION IN AN INTACT LEAF BETWEEN THE TWO PHOTOSYSTEMS OF PHOTOSYNTHESIS

CHANGES IN ABSORPTION CROSS-SECTIONS FOLLOWING STATE 1–STATE 2 TRANSITIONS

ORA CANAANI and SHMUEL MALKIN

The Weizmann Institute of Science, Rehovot 76100 (Israel)

(Received December 15th, 1983)

Key words: Oxygen evolution; State transition; Photosynthesis; Photosystem; Light excitation; Photoacoustic spectroscopy

Using the photoacoustic technique, state 1–state 2 transitions were studied in an intact leaf by direct monitoring of modulated oxygen evolution, excited by modulated light. States 1 and 2 were characterized by the extent of immediate enhancement of the modulated oxygen evolution – 'Emerson enhancement' – and the concomitant fluorescence quenching, resulting from the addition of continuous far-red light (greater than 700 nm), absorbed primarily in Photosystem I (light 1). The extent of Emerson enhancement as well as the saturation curve of this effect by far-red light are very sensitive and quantitative indicators for the ratio of light excitation distributed between Photosystems I and II. The enhancement ratios at 650 nm light, a typical light 2, were in a range 1.4–1.8 in state 1, while values as low as 1.06 were observed in state 2. During the transition from state 2 to state 1, monitored in presence of modulated light 2 and background continuous light 1, the modulated oxygen yield increased considerably, indicating a major increase in excitation flux into Photosystem II. Conversely, with modulated light 2 alone in state 1, the modulated oxygen evolution yield was smaller than in state 2, indicating a decrease of the excitation flux in Photosystem I. In a typical example, of the transition to state 1, the fraction of light absorbed by Photosystem II, β, increased from 0.46 to 0.64, while that absorbed by Photosystem II, α, decreased from 0.43 to 0.36. State 1–state 2 transitions, thus, reflect reciprocal changes in the cross-sections of the two photosystems for light absorption. There is no evidence for the operation of a 'spill-over' mechanism. The enhancement effect displayed maxima at 480 and 650 nm, related to chlorophyll-*b* absorption, as well as another band at 500–550 nm. In a chlorophyll-*b*-less barley mutant, state 1–state 2 transitions, as monitored by modulated oxygen evolution, were absent, and the resulting enhancement corresponded to state 2. These observations are consistent with the model that the light-harvesting chlorophyll-*a*/*b* complex plays a role in regulating the distribution of light to the photosystems. It is probable that this complex migrates reversibly in the thylakoid membrane in such a way that it is mainly associated with Photosystem II in state 1, but is more evenly distributed in the two photosystems in state 2.

Introduction

The initial distribution of light excitation between the two photosystems of photosynthesis depends on the relative cross-sections for absorption of each photosystem at any particular wavelength, and is usually unbalanced; in higher plants and green algae Photosystem II (PS II) absorbs more light than Photosystem I (PS I), over most of the spectral range ($\lambda \leqslant 680$ nm) but considerably less at longer wavelengths ($\lambda \geqslant 690$ nm). At limiting light intensities, noncyclic electron flow, which

requires the tandem operation of both photosystems is limited by the particular photosystem having the lower absorption cross-section (i.e., by PS I at $\lambda \leqslant 680$ nm and by PS II in the far-red region). In response to the spectral composition of the prevailing illumination, there is a physiological adjustment, completed within a relatively short time (minutes), towards one of two possible states of light distribution: state 1, with unequal light distribution, as described above, and state 2, approaching a much more equal distribution over the short wavelength range [1–5]. The induction of a state transition depends in a quantitative manner on the surplus of excitation in one photosystem relative to the other. State 1 results from over-excitation of PS I, by light mainly absorbed in Photosystem I (light 1) and state 2 results from over-excitation of PS II by short wavelength light (light 2). State 1–state 2 transitions were first reported in algae on basis of measurements of slow changes in the quantum yields of chlorophyll fluorescence and oxygen evolution [1] and by low (77 K) tempreature fluorescence spectroscopy [2].

Experiments on isolated broken chloroplasts indicate two alternative phenomenological ways in which the light distribution between the two photosystems can be affected: (a) Addition of cations reversibly increase the apparent rate of excitation of PS II and decrease that of PS I [6,7]; (b) phosphorylation of membrane proteins, notably that of the light harvesting chlorophyll-*a*/*b* protein complex (LHC), [8,9], causes a decrease of PS II activity parallel to an increase in that of PS I [10–14]. This effect was reversed in the dark or by far-red light as under these conditions the membranes were dephosphorylated [47].

Changes in light distribution can occur by two different mechanistic options [6]: (a) spill-over, which implies, by definition, a unidirectional transfer of excitation energy from PS II to PS I, in competition with the primary photochemical act in PS II. It, thus, requires a close distance between the specific antennae of the two photosystems and depends on the state of the reaction centers of PS II, having significantly higher probability as these centers are photochemically 'closed'. The term spill-over was introduced to distinguish it from the 'separate-package' model where no such excitation transfer exists [15]. (b) Change in the direct absorption cross-section of each of the two photosystems [1], brought about by changes in pigment distribution. In contrast to the induction of a spill-over mechanism, the change in absorption cross-section requires that pigment antennae themselves change their distribution, with no particular limitation on the distance between the two photosystems and the state of the reaction centers. All the above options can be quantitated by introducing the relative absorption cross-sections α and β – the fraction of absorbed light delivered initially to PS I and PS II, respectively, and the spill-over probability, ψ. Changes in these parameters were previously mainly analyzed by changes in fluorescence parameters and partial activities of PS I or PS II, [6,16–19].

Considerable evidence exists showing that the transition from low to high cation environment in isolated thylakoids brings about a transition from spill-over to separate package [6,7]. On the other hand, phosphorylation of isolated thylakoids causes, very probably, changes in the absorption cross-section of each of the photosystems such that β decreases and α increases [10,11,13]. The situation in-vivo is not clear, since the mechanism involved in state 1 $\leftrightarrow$ state 2 transitions is not yet completely elucidated. There are conflicting conclusions whether these transitions are mainly associated with reciprocal changes in α and β, as for example Bonaventura and Myers suggested, for *Chlorella pyrenoidosa* [1] or whether they are associated with changes in the energy transfer probability, as Ley and Butler reported for the red algae *Porphyridium cruentum* [19,20]. Recently, evidence was reported showing that, at least in green organisms, these transitions are associated with the change in the phosphorylation level of thylakoid proteins [21,22] with possible implications that absorption cross-sections are affected.

We consider fluorescence measurements as equivocal and not capable of yielding quantitative results in complex situations due to the existence of a large number of parameters affecting the fluorescence in different ways [23]. Our approach to the problem is to study directly the oxygen evolution yield in light 2, of short wavelength, its enhancement by far-red light 1, which allows a direct quantitation of the cross-section parameters. We use intact leaves of higher plants as a typical

highly developed photosynthetic organism. In such a case, it was shown that the photoacoustic method is a very suitable tool [24] for studying photosynthetic activities, particularly, since it involves a modulation technique, similar to the modulated oxygen rate electrode [25]. State 1 ↔ state 2 transitions in a higher plant leaf were previously characterized by observing the effect of light 1 on the fluorescence quenching [26], as well as by our previous preliminary work [27]. The present report is a comprehensive extension of the above work with a thorough study on the light distribution between the photosystems in states 1 and 2, and during the transition between them. It is shown that changes in the distribution of excitation energy during state 1 ↔ state 2 transitions are significant and are consistent with changes in the absorption cross-sections of the two photosystems rather than with changes in the spill-over from PS II to PS I.

Materials and Methods

Plant material. Tobacco leaves (*Nicotiana tobacum* L. var. Xanthi) were the standard material mostly used for these experiments. Occasionally, spinach leaves were used for comparison. Certain experiments were performed on barley (*Hardeum vulgare* var. Lyon) and the mutant of barley lacking chlorophyll *b* [28]. The plants were grown outdoors. Small round sections of diameter 1 cm were cut and used.

Photoacoustic and fluorescence set-up. In photoacoustic measurements of a leaf, absorbed modulated light causes the release of both modulated heat and modulated oxygen evolution [24]. Both heat and oxygen diffuse from the chloroplasts to the cell surface and cause a layer of the inner air phase near the surface to expand and contract periodically, thus, creating an acoustic wave, which propagates outside the leaf. The acoustic signal is detected by a microphone (Knowles), whose current is preamplified and processed by a lock-in amplifier (Ortholock 9502, Brookdeal) for its in-phase and quadrature components. At low modulation frequency (no greater than approx. 100 Hz), a very large part of the photoacoustic signal arises from modulated photosynthetic oxygen evolution [24,29]. By using a background light of constant and high intensity, in addition to the modulated light, photosynthesis is saturated, and the modulated oxygen evolution is eliminated. The remaining photoacoustic signal is then directly proportional to the heat flux due to an approximately full radiationless conversion of the absorbed modulated light. The last signal, after a correction due to the 'photochemical loss' (i.e., the fraction of the photon energy stored by the photochemical reactions [30]) is subtracted vectorially from the total signal to yield the oxygen evolution signal [29]. The photochemical-loss is estimated separately from high frequency at around 400 Hz, at which modulated oxygen evolution is negligible [24,29].

A detailed description of our photoacoustic apparatus, capable also of monitoring modulated fluorescence from the sample, is given in [24]. Modulated light was provided from a 450 W d.c. xenon lamp and a monochromator (Bausch and Lomb, 10 nm bandpass). Modulation was obtained by passing the light through rotating wheel chopper (Laser precision) allowing the selection of any convenient frequency. Background nonmodulated light was obtained from a d.c. operated projector equipped with an appropriate optical filter. This arrangement provided either background far-red (710 nm) used as light 1, or a strong, photosynthetically saturating, wide band (400–600 nm) light. The modulated and background lights were combined by using a triple branched light guide having a common end. The third branch was used to pass modulated fluorescence from the sample into an a.c. photovoltaic detector (EG and G). Fluorescence emission was passed through a 680 nm interference filter and further blocked by 645 nm longpass (Schott) and 700 nm shortpass filters (Interference-Ditric optic), so that none of the exciting background lights could interfere. The modulated fluorescence was processed through a second lock-in amplifier (PAR 128). The three signals: the in-phase and quadrature components of the photoacoustic response, and the fluorescence amplitude, were recorded simultaneously as functions of the time. Light intensities were measured by a bolometer (Yellow springs Instruments), placing the detector in the photoacoustic cavity.

Results

The photoacoustic technique enables us to measure the relative absorbance of the leaf, together with the relative quantum yield of both oxygen evolution and energy storage [24,30] in a single experimental run and with the same sample (Fig. 1). The photoacoustic oxygen evolution signal amplitude A_{OX} is proportional to ϕi, where ϕ is the quantum yield and i the absorbed modulated light intensity. The photothermal signal A_{PT} which is the resulting photoacoustic signal in the presence of saturating background light is proportional to $h\nu i$, where $h\nu$ is the photon energy. Thus, the ratio $(A_{OX}/A_{PT})(\lambda)^{-1}$ is proportional to the quantum yield of oxygen evolution. Scanning the latter ratio vs. the wavelength gives the relative quantum yield spectrum (Fig. 1a). It has a broad maximum in the red region, 600–680 nm, and a smaller maximum in the blue region around 440 nm. Most importantly, at the far-red region 680–720 nm where chlorophyll absorbance is still high, a sharp drop is noticed. This is the well known 'red-drop' phenomenon, previously observed by other methods in algae and chloroplasts [31,32]. The relative percent absorbance of the leaf can be obtained from the ratio of the photothermal signal A_{PT} to the energy flux of the incident light. The spectral shape shown in Fig. 1b, is typical for a leaf, a highly scattering sample, and shows clearly the absorption of chlorophyll with the Soret band at 440 nm more intense than the red absorption peak at 680 nm. This spectrum is similar in its gross features to previously published ones, obtained conventionally [33].

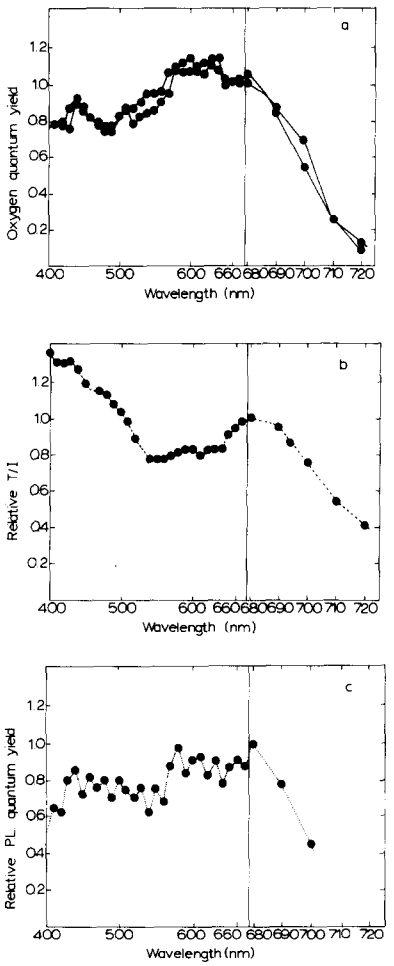

Fig. 1. (a) Relative quantum yield of oxygen evolution (A_{OX}/A_{PT} divided by λ) from an intact tobacco leaf. (Two examples of two leaves are shown: in one, the yield was normalized to 1 at 680; the other one is relative to the first.) Modulation frequency, 22 Hz. (b) Relative percent absorbance of the leaf measured photoacoustically as A_{PT}/I, where I is the incident light intensity. (C) Quantum yield of energy storage, calculated as the photochemical loss (P.L.) divided by λ (in μm). Modulation frequency, 415 Hz.

The photoacoustic method also provides a unique possibility of measuring the energy stored in photochemical intermediates formed in the photosynthetic process [30]. At sufficiently high modulation frequency, the oxygen signal disappears, and the ratio $(A^* - A)/A^*$ (where A and A^* are the signal amplitudes with and without background light) indicates the photochemical loss, L [24,29], is proportional to $\phi' \Delta E/h\nu$, where ΔE is the energy gain by products of the photosynthetic reaction per reaction unit, and ϕ' is the quantum yield. Thus, the quantum yield is proportional to L/λ. This quantum yield of energy storage is not necessarily equal, or parallel, to the quantum yield of oxygen evolution; the later reflects that part of the photosynthetic reaction which is due to non-cyclic electron transport only, while the former may indicate the additional participation of a cyclic electron transport. The quantum yield of energy storage is shown in Fig. 1c, with the red drop also noticed here. It also shows the two peaks in the red and the blue, with higher efficiency in the red region 580–680 nm, compared to the blue region around 440 nm.

Fig. 2 illustrates the increase in the modulated yield of oxygen evolution, excited by light 2 (in this particular case, broad band 400–600 nm), by the addition of nonmodulated light 1 (710 nm) background. This is a demonstration of Emerson enhancement [34]. This and the simultaneous fluorescence quenching (Refs. 22, 26 and 27; cf. also later) are indications of the imbalance of photon delivery to the two photosystems in light 2, due to excess excitation in PS II. Explanation of this effect, in relation to the way the experiment is performed here, is as follows: initially, the reaction centers of PS II are partially closed, as the net rate through the two photosystems is limited by the smaller light absorption in PS I. With excess light 1, however, PS II reaction centers become open by oxidation of PS II electron acceptor by PS I, which results in maximal modulated oxygen evolution yield and minimal fluorescence (cf. Appendix). The enhancement ratio E was calculated as the ratio of the yields of oxygen evolution in presence and absence of the far-red background light.

The saturation curves of both Emerson enhancement and fluorescence quenching (i.e., their dependence on the intensity I of the background light-1) appear to be very similar, as shown in Fig. 3. The data in this particular experiment were obtained in state 2 (cf. later). Low intensities of far-red light are sufficient to saturate the enhancement effect, indicating that initially there is only a slight imbalance between the photosystems in favor of PS II. This is consistent with the low value of

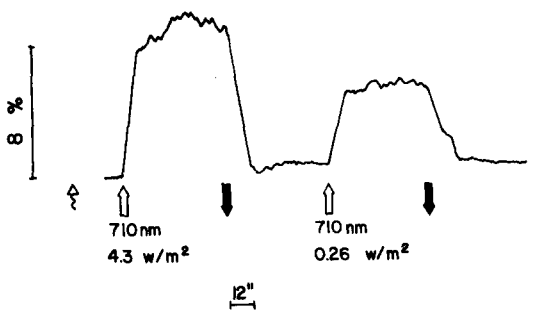

Fig. 2. Emerson enhancement of modulated oxygen evolution caused by addition of far-red (710 nm) constant background light at two intensities, as indicated. Oxygen evolution (monitored by photoacoustic signal at 22 Hz) was measured with modulated light 2 (broad band 400–600 nm, 5.5 W/m^2) after adaptation to state 2.

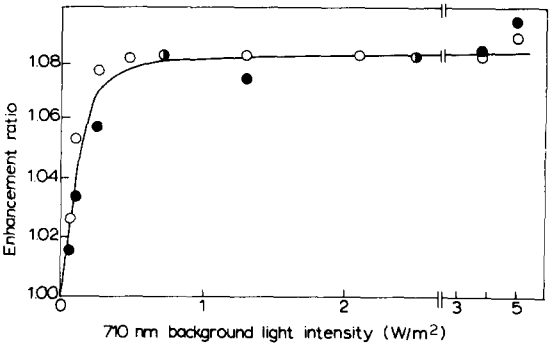

Fig. 3. Intensity dependence of the enhancement of the oxygen evolution (○——○) and the fluorescence quenching (●——●) induced by far-red light, measured at state 2. Modulated light, 400–600 nm, 5.5 W/m^2, was used for both adaptation and measurement.

the enhancement ratio for this case (cf. later). The saturation curve for enhancement is expected to depend on the ratio of the intensities of the two lights used (cf. Appendix). This is exemplified by Fig. 4. Thus, in the linear region of the saturation curve, an increase of modulated light-2 intensity requires proportionally higher intensity of light-1 background to achieve the same enhancement. This result is typical for an effect rooted in an imbalance between the two lights, and was noticed previously [35]. In this, and the following experiments, light intensities are expressed in terms of

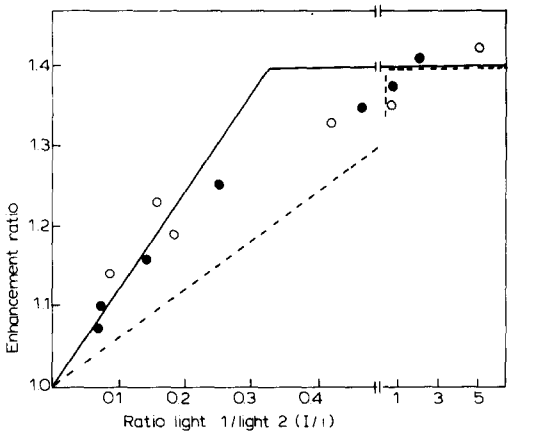

Fig. 4. Emerson enhancement in state 1 as function of the ratio of the intensities of light 1 (I) to light 2 (i). Two light intensities of modulated light 2 (650 nm) were used: 5.2 (●) and 2.2 (○) W/m^2. The lines are theoretical calculations corresponding to the separate-package (———) and spill-over (- - - - -) models (cf. text).

(relative) absorbed fluxes, by comparing the corresponding photothermal photoacoustic signals at any wavelength. The absorbed intensity of the far-red background light is estimated separately, in a similar way, from the photothermal effect induced by the same light when it is modulated.

The enhancement saturation curves shown in fig. 4 were obtained for state 1 and will be discussed here in detail, in terms of the analysis presented in the Appendix. The fractions of light distributed to PS I and PS II are denoted by α and β, respectively. From the maximal enhancement ratio (1.40), the value of β is calculated to be 0.58, assuming no spill-over, and $\alpha + \beta = 1$. We measured separately the photothermal signal and the ratio of the oxygen and photothermal signals for the far-red light (710 nm) when it was modulated, allowing us to estimate the absorbed intensity and the quantum yield of oxygen evolution for this particular far-red wavelength. From the quantum yield obtained at 710 nm (0.6 of the value observed at 640 nm) it is concluded that $\beta' = 0.28$ and $\alpha' = 0.72$. The calculated initial slope of the enhancement saturation curve should be accordingly: $(0.72/0.42) - (0.28/0.58) = 1.23$. The experimental value is 1.15, in a very reasonable agreement. If a spill-over model is assumed, with the same data as above, $\beta = 0.68$ and the predicted slope is $0.72 - (0.32 \times 0.28/0.68) = 0.59$. Thus, the saturation curve of Fig. 4 is in a quantitative agreement with the separate package model, rather than with the spill-over model. It turns out that the enhancement saturation curve is a sensitive indicator for the selection of the right model. Fig. 4 shows the theoretically calculated enhancement saturation curves, for both models.

The quantum yield spectrum of PS I for the enhancement effect is shown in Fig. 5. In this experiment, oxygen evolution yield was monitored with 640 nm modulated light. An enhancement saturation curve was obtained at each different wavelength of the background light, as in Figs. 3 and 4. The relative quantum yield was calculated as the slope of the enhancement saturation curve in the linear region. This spectrum has a maximum at 700–720 nm and is zero at light-2 region (650–680 nm, data not shown) as expected. It, thus, corresponds to light 1 spectral region, where the red-drop occurs. The loss of the far-red efficiency at $\lambda \gtrsim 720$ nm could be due partly to a loss in quantum efficiency (resulting perhaps from the requirement of an 'uphill' excitation transfer to the reaction center). Otherwise, it could indicate that at these longer wavelengths some far-red light is distributed also to PS II, although the distribution to PS I still dominates. Such a decrease in the far edge of the far-red region was noted previously for algal systems [34] and in the quantum yield of electron transfer from a donor system to NADP in isolated chloroplasts [32]. However, the pronounced decrease in Fig. 5 could perhaps also involve some artifacts due to an irrelevant background photoacoustic signal which could cause an apparent increase in the absorbed light intensity, at wavelengths of very weak absorption.

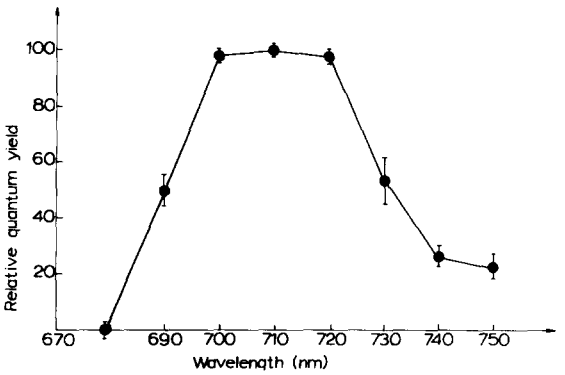

Fig. 5. Relative quantum yield spectrum of the Emerson enhancement effect, calculated from the initial slope of the far-red saturation curves, as in Figs. 3 and 4. Modulated light was 640 nm, 7.4 W/m^2. Modulation frequency, 22 Hz. The spectrum refers to absorbed quanta obtained from the photothermal contribution to the photoacoustic signal [29].

State 1–state 2 transitions

Prolonged illumination (approx. 10 min) with modulated light 2 results in adaptation of the leaf to state 2 (Fig. 6, here light 2 was 650 nm). State 2 is characterized by a rather small enhancement ratio, E, of 1.065, and a correspondingly very small decrease in the fluorescence yield. With the addition of nonmodulated 710 nm background light for a long period, a gradual slow increase in the oxygen evolution yield and a concomitant decrease in the fluorescence occur. This adaptation process corresponds to the transition from state 2 to state 1, and usually takes several minutes. Upon

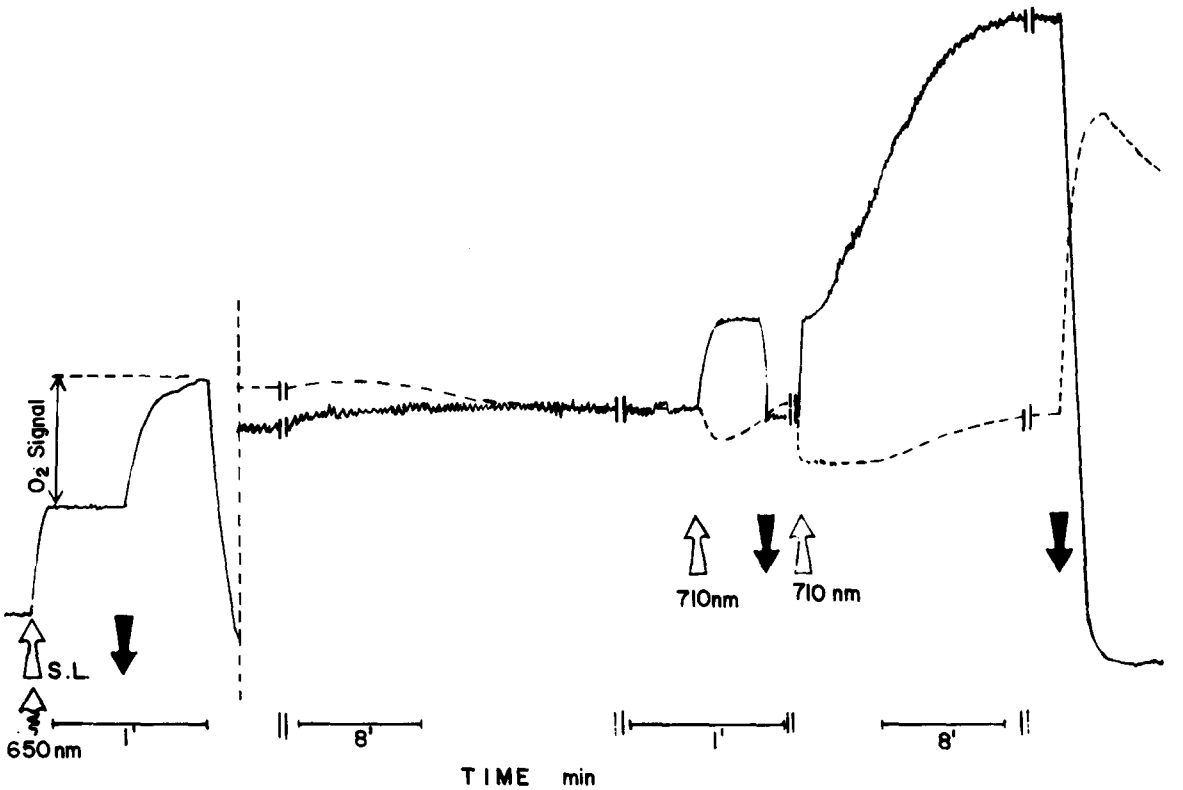

Fig. 6. State 1–state 2 transitions in an intact leaf, monitored by slow changes in the far-red induced Emerson enhancement (———) and fluorescence quenching (- - - - -). Modulated light, 650 nm, 5.2 W/m^2. Far-red light, 710 nm, 20 W/m^2. Modulation frequency 22 Hz. The photoacoustic signal in the presence of saturating background light (S.L.) of 400–600 nm, 400 W/m^2, represents the zero level for oxygen evolution. In turning off the S.L., the oxygen signal increased to a steady-state level. Using zero suppression with the lock-in amplifier, as indicated by the vertical dashed line, the signal was amplified by a factor of 10 and the adaptation experiment was started.

removal of far-red light, an immediate large increase in the fluorescence and a large decrease in the oxygen photoacoustic signals are observed. This phenomenon is immediately reversed upon a momentary addition of the far-red light, indicating a large Emerson enhancement ratio (1.76 in this particular example), concomitant with a large fluorescence quenching. Such state 1–state 2 transition cycles could be repeated several times.

In the analysis of Fig. 6, we will compare the light distribution ratios in states 1 and 2. From this figure, it is clear that the transition from state 2 to state 1, in the presence of excess far-red background light, is characterized by a considerable increase in the level of modulated oxygen evolution. According to the Appendix, this level is proportional to β, the fraction of excitation channeled into PS II from the modulated light. This effect demonstrates that β is changing during the transition and allows calculation of the ratio β(state 1)/β(state 2), which in this particular experiment is equal to 1.38. This change in β demonstrates a mechanism in which the cross-section of the two photosystems for light absorption is changing considerably. From the value of the enhancement ratio in state 1 (1.76), assuming no spill-over, it is calculated that β is equal to 0.64 ($\alpha = 0.36$) in state 1. From the above ratio of β in the two states, it follows that in state 2, $\beta = 0.46$. From the enhancement ratio (equal to β/α) it follows that α in state 2 is equal to 0.43. If spill-over is assumed to occur in state 2, α is calculated to be somewhat smaller (0.40). In both cases, there is some loss of excitation in state 2 (11–14%) judged from the sum $\alpha + \beta$. In conclusion, state 1 represents a situation where the initial

distribution of light into the two photosystems is considerably far from balance. In the transition to state 2, PS II loses part of its absorption cross-section while PS I gains part from what has been lost by PS II. Thus, a near balance of the absorption cross-sections is achieved. Whether or not there is a spill-over mechanism in states 1 or 2 is actually a separate question. As shown in the Appendix, even when the spill-over mechanism operates, an initially unbalanced distribution of excitation in the two photosystems will result in a significant Emerson enhancement. According to the saturation curve of the enhancement, we arrived at the conclusion that there is no spill-over in state 1. In state 2, since the absorption cross-sections are nearly equal there is no functional need for spill-over.

In the various experiments with state transitions, the enhancement ratios in state 1 varied from 1.2 to 1.8. This was apparently dependent on the ratio of light 1 and 2 during the adaptation process. We did not use 'pure' light 1 to affect the transition to state 1 since under conditions of low intensities, additional effects take place, e.g., adaptation to a 'low-light' state (cf. Ref. 27). In order to obtain a noticeable enhancement in state 1, the ratio of the two lights in causing the transition should be at least 2 : 1 richer in light 1.

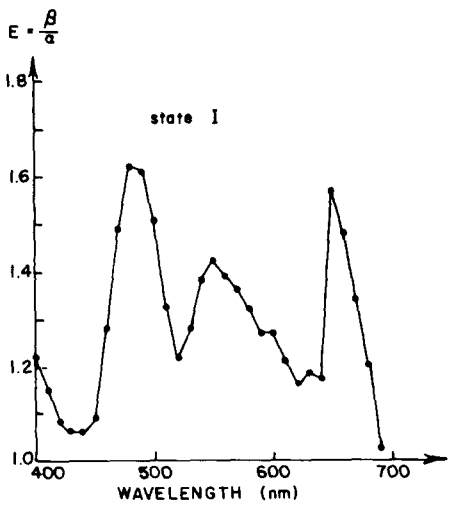

Fig. 7. Emerson enhancement spectrum as function of light 2 wavelength, in state 1 and with saturating light 1 (710 nm, 18 W/m^2). It was ascertained that state 1 was obtained at each new light 2 wavelength by using 10 min preillumination with excess light 1. Modulation frequency, 22 Hz.

TABLE I

Emerson enhancement ratio (E) of oxygen evolution and the extent of fluorescence quenching ($\Delta F/F$) induced by light 1 background in consecutive states 2 and 1 in intact leaves of barley wild type (w.t.) and in chlorophyll-*b*-less barley mutant.

Species	Adaptation condition	E	$\Delta F/F$
Barley w.t.	state 2	1.13	0.025
	state 1	1.22	0.100
Barley mutant	state 2	1.10	0.020
	state 2	1.10	0.020

Emerson enhancement spectrum

The maximum enhancement, obtained with excess far-red light depends on the ratio of distributions of the modulated light 2 (cf. Appendix) and, hence, is wavelength-dependent. A demonstration of such enhancement spectrum, obtained with saturating far-red light, is shown in Fig. 7. The enhancement spectrum shows peaks at 480–485 and 650–655 nm, probably due to the dominant absorption of chlorophyll *b*, which is present mainly in PS II. There is a crossover (i.e., transition to light 1 region) at 680–685 nm. The absorbance of the two photosystems is also nearly equal at the blue absorption peak of chlorophyll *a*, 440 nm, thus yielding only a small Emerson enhancement ratio. Interestingly, at the green spectral region, around 550 nm, there is an additional increased absorption of PS II relative to PS I, leading to large enhancement in this particular region. The increased enhancement at 550 nm is probably again related to a higher relative absorbance of chlorophyll *b* relative to chlorophyll *a*, although neither of them shows any prominent absorption in this region. A similar enhancement spectrum was obtained with spinach leaves (data not shown). The enhancement spectrum shown in Fig. 7 was obtained in state 1. A qualitatively similar spectrum was achieved in state 2, although with considerably reduced values (data not shown). Similar spectral regions of increased PS II activity were noted by Joliot [36].

State transitions in barley and its chlorophyll-b-less mutant

It was of interest to experiment with a chlorina mutant of barley which lacks chlorophyll *b* and is specifically deficient in functional LHC [37]. We measured state 1–state 2 transitions in normal barley, and compared them to the barley mutant (Table I). In a normal barley leaf, as in the other species tested, the enhancement in oxygen evolution and fluorescence quenching were minimal ($E = 1.13$) in state 2 and maximum ($E = 1.22$) in state 1. In the barley mutant, however, there was only one state, similar to state 2 ($E = 1.10$), and no special adaptation to additional excess far-red light was present. We also repeated parallel measurements using fluorescence with essentially the same conclusions. Far-red light induced fluorescence quenching was identical, either after prolonged irradiation with 650 nm, or following prolonged illumination with 710 nm. Similar fluorescence results were reported previously by Chow et al. [26]. An analysis of low temperature fluorescence induction of thylakoids isolated from this barley mutant [38] indicated no changes in any of the parameters α, β or ψ due to either cation addition or depletion or due to phosphorylation of membrane proteins, other than LHC.

Discussion

Photoacoustic measurements on leaves are rapid and sensitive, and give an insight into photochemical energy storage and oxygen evolution [24]. We have used the technique to investigate light distribution between the two photosystems. Similar observations mainly by measurements of Emerson enhancement and quantum yields of partial reactions, were reported long ago on algal systems and isolated chloroplasts, but there are very few experiments reported using leaves, due to the previous lack of fast and sensitive methods for measuring gross photosynthesis. Detection of state 1–state 2 in an intact leaf by fluorimetry [26], does not give quantitative information about photosynthetic efficiency. There is a single report on the change of steady-state oxygen evolution yield in an intact leaf, measured by the conventional Clark type oxygen electrode, caused by changing illumination conditions, which was also correlated with transitions from granular to more homogenous chloroplasts [39].

In this work, it is demonstrated that changes in absorption cross-sections of each of the photosystems is the major event leading to the state 1–state 2 transitions in the intact leaf. We have shown that Emerson enhancement in state 1 may reach levels as high as 1.8. In this case, light 2 was 650 nm and the calculated distribution ratios were 0.64 and 0.36 for PS II and PS I, respectively. On the other hand, in a typical state 2, or in the chlorophyll-*b*-less barley mutant, the typical enhancement ratio was about 1.05, implying nearly equal distribution ratios (0.51 and 0.49, respectively, for light 2 of 650 nm). The difference between the two states is consistent with significant reciprocal changes in the antennae of the two photosystems, involving migration of pigments from PS II to PS I, during the transition from state 1 to state 2, and vice versa. With regard to the present literature and according to the model of Andersson [40] and Andersson and Anderson [41], there is indeed a significant spatial separation between the two photosystems; PS II, is mainly located in the appressed regions of the membranes and PS I, is located in the nonappressed regions and in the stroma lamellae. Our results, together with all the above studies, indicate at least two requirements needed to observe transition to state 1: the presence of functional LHC and its capability of being phosphorylated [22]. LHC is considered mobile, reversibly migrating between the two photosystems. A possible molecular mechanism for the movement of the LHC, was described by Barber [42]. This model suggests the separation of phosphorylated LHC from PS II, at least to some extent, and its diffusion to the nonappressed regions, where it may become associated with PS I. This model is supported by freeze-fracture electron-microscopic observations of corresponding changes in the distribution of particles, believed to be images of the LHC, between grana and stroma lamellae regions, as a result of the LHC phosphorylation [43]. Similar conclusion was derived from the distribution of label of ^{32}P in grana and stroma in phosphorylated vs. nonphosphorylated membranes [44].

Possible exceptions to the above model are red and blue-green algae, which also exhibit phenom-

ena similar to state 1 ↔ state 2 transitions [3,4,19,20]. These organisms do not contain LHC and the phosphorylation mechanism in general was questioned in them [4,5,45]. In the red algae *Porphyridium cruentum,* Ley and Butler [19,20] specifically reported that states 1 and 2 differed by spill-over only. Indeed, these organisms must have different mechanisms for regulation of light distribution. They contain large complexes, phycobilisomes, attached to the outer surface of the thylakoid membrane as their major accessory antennae pigments. On the other hand, it was claimed that in a mutant of a green alga *Scenedesmus obliquus,* which lacks LHC, state 1–state 2 transitions still did occur [5]. Inspection of the data, however, particularly the fluorescence induction curves, leads one to believe that also in this case there is a change towards more spill-over in state 2, rather than a change in absorption cross-sections. Thus, in this alga the adaptation to different light regimes is of a different nature than in an intact leaf. Also, in this regard, it must be stressed that fluorescence phenomena are complicated and influenced by factors other than light distribution. Therefore, the 'states', as studied above which were mainly defined by fluorescence parameters, may represent also other types of phenomena. For algal suspension the best method to study state transitions, should be by following oxygen evolution (e.g., by using the modulated oxygen electrode [25]) measurements of Emerson enhancement.

The function served by the state transitions is not entirely resolved. Given the fact that only PS I contains far-red absorbing pigments, it is advantageous to have an even distribution of shorter wavelength light when this light is present in abundance, compared to the far-red light. Conversely, it is an advantage to have a distribution of short-wavelength light much in favor of PS II when there is ample ambient far-red light compared to short-wavelength light. The last situation may prevail inside a deep foliage [46]. With this teleological reasoning, one still must explain why far-red pigments form an indispensible part of PS I, and whether they serve a particular role which is important to the special functional properties of this photosystem, or if they just remained through evolution.

Appendix

Calculation of the Emerson enhancement effect

Let α and β be the fractions of the absorbed modulated light, distributed initially to Photosystems I and II, respectively. We assume optimal photochemical efficiency of an 'open' reaction center, for each of the photosystems. The modulated rate of oxygen evolution is equal to $f\beta i$, where f is a loss factor due to the partial closure of PS II reaction centers (cf. Ref. 42) and i is the intensity of modulated light 2. For light 2, $\beta > \alpha$ and $f < 1$. In the separate package model, the required balance of the nonmodulated part of the electron transport rate through the photosystems imposes: $f\beta i = \alpha i$, hence $f = \alpha/\beta$ and the modulated rate is equal to αi. In the spill-over model, excitation is funneled to PS I in competition to the partial closure of PS II reaction centers, a process balanced when the excitation is distributed evenly. The modulated rate is then equal to $(\alpha + \beta)i/2$. This result is also consistent with a spill-over excitation transfer rate given by $(1-f)\beta i$, since the equation of balanced rates: $f\beta i = \alpha i + (1-f)\beta i$ imposes $f = (\alpha + \beta)/2\beta$. With excess continuous far-red light, PS II is operating optimally, $f = 1$ and the modulated rate is equal to βi. The maximal enhancement ratio is, therefore, β/α for the separate-package case, and $2\beta/(\alpha + \beta)$ for the spill-over case. In the main text we assumed also $\alpha + \beta = 1$ for state 1. In state 2, however, there was some loss in the sum of the absorption cross-sections, and $\alpha + \beta < 1$.

Of equal importance is the initial slope of the Emerson enhancement saturation curve, or equivalently the minimum intensity of light 1 sufficient to bring about the maximum enhancement effect. This is calculated as follows: in the separate-package model, the balanced nonmodulated rate requires: $f(\beta i + \beta' I) = \alpha i + \alpha' I$, where i is again the average intensity of modulated light 2 and I is the continuous intensity of light 1. The prime refers to the distribution parameters of light 1. Hence: $f = (\alpha i + \alpha' I)/(\beta i + \beta' I)$ (as long as this ratio is less than 1, otherwise $f = 1$), the modulated rate is $\beta i(\alpha i + \alpha' I)/(\beta i + \beta' I)$ and the enhancement ratio is:

$$E = \frac{\beta}{\alpha} \frac{\alpha i + \alpha' I}{\beta i + \beta' I} \tag{1}$$

(as long as the second factor remains smaller than 1). From this equation, the linear part of E, for small I/i, is approximated by:

$$E = 1 + \left(\frac{\alpha'}{\alpha} - \frac{\beta'}{\beta}\right)\frac{I}{i} \quad (2)$$

In the spill-over model, the balanced nonmodulated rate equation is: $f(\beta i + \beta' I) = \alpha i + \alpha' I + (1 - f)(\beta i + \beta' I)$, hence: $f = (\alpha + \beta)i + (\alpha' + \beta')I / 2(\beta i + \beta' I)$ with the modulated rate equal to $\beta f i$, the enhancement ratio is calculated to be:

$$E = \frac{2\beta}{\alpha + \beta} \cdot \frac{(\alpha + \beta)i + (\alpha' + \beta')I}{2(\beta i + \beta' I)} \quad (3)$$

(as long as the second term remains smaller than 1). The linear part of E, for small I, is approximated by:

$$E = 1 + \frac{\beta\alpha' - \alpha\beta'}{\beta(\alpha + \beta)} \cdot \frac{I}{i} \quad (4)$$

Acknowledgements

This research was supported in part by the Israel Academy of Science and Humanities. The authors wish to thank D. Cahen and J. Barber for a critical reading of the manuscript.

References

1 Bonaventura, C. and Myers, J. (1969) Biochim. Biophys. Acta 189, 366–383
2 Murata, N. (1969) Biochim. Biophys. Acta 172, 242–251
3 Reid, A. and Reinhardt, B. (1980) Biochim. Biophys. Acta 592, 76–86
4 Fork, D.C. and Satoh, K. (1983) Photochem. Photobiol. 37, 421–428
5 Satoh, K. and Fork, D.C. (1983) Photochem. Photobiol. 37, 429–434
6 Williams, P. (1977) in Topics in Photosynthesis, Vol. 2, Primary Processes in Photosynthesis, pp. 99–147, Elsevier, Amsterdam
7 Briantais, J.M., Vernotte, C. and Maison, B. (1982) Phys. Véget. 20, 111–122
8 Bennett, J. (1977) Nature 269, 344–346
9 Bennett, J. (1979) Eur. J. Biochem. 69, 133–137
10 Bennett, J., Steinback, K.E. and arntzen, C.F. (1980) Proc. Natl. Acad. Sci. USA 77, 5253–5257
11 Horton, P. and Black, M.T. (1981) Biochim. Biophys. Acta 635, 53–62
12 Steinback, K.E., Bose, S. and Kyle, D.J. (1982) Archiv. Biochem. Biophys. 216, 356–361
13 Farchaus, J.W., Widger, W.R., Cramer, W.A. and Dilley, R.A. (1982) Arch. Biochem. Biophys. 217, 362–367
14 Horton, P. and Black, M.T. (1980) FEBS Lett. 119, 141–144
15 Myers, J. (1963) in Photosynthetic Mechanisms of Green Plants (Kok, B. and Jagendorf, A.T., eds.), pp. 301–317, publ. 1145, Natl. Acad. Sci.-Natl. Res. Counc. Washington D.C.
16 Butler, W.L. and Kitajima, M. (1975) Biochim. Biophys. Acta 396, 72–85
17 Butler, W.L. (1977) in Encyclopedia of Plant Physiology, New Series (Trebst, A. and Avron, M., eds.), Vol. 5, pp. 149–167, Springer-Verlag, Berlin
18 Butler, W.L. and Kitajima, M. (1975) Biochim. Biophys. Acta 396, 72–85
19 Ley, A.C. and Butler, W.L. (1977) in Photosynthetic Organelles, Spec. Issue, Plant Cell Physiol. pp. 33–46
20 Ley, A.C. and Butler, W.L. (1980) Biochim. Biophys. Acta 592, 349–363
21 Wollman, F.A. and Deleplaire, P. (1984) J. Cell Biol. 98, 1–7
22 Canaani, O., Barber, J. and Malkin, S. (1984) Proc. Natl. Acad. Sci. USA 81, 1614–1618
23 Lavorel, J. and Etienne, A.L. (1977) in Topics in Photosynthesis, Vol. 2, Primary Processes in Photosynthesis, pp. 205–268, Elsevier, Amsterdam
24 Bults, G., Horwitz, B.A., Malkin, S. and Cahen, D. (1982) Biochim. Biophys. Acta 679, 452–465
25 Joliot, P., Joliot, A. and Kok, B. (1968) Biochim. Biophys. Acta 153, 635–652
26 Chow, W.S., Telfer, A., Chapman, D.J. and Barber, J. (1981) Biochim. Biophys. Acta 638, 60–68
27 Canaani, O., Cahen, D. and Malkin, S. (1982) FEBS Lett. 150, 142–146
28 Highkin, H.R. (1950) Plant Physiol. 25, 294–306
29 Poulet, P., Cahen, D. and Malkin, S. (1983) Biochim. Biophys. Acta 724, 433–446
30 Malkin, S. and Cahen, D. (1979) Photochem. Photobiol. 29, 803–813
31 Emerson, R. and Lewis, C.M. (1943) Am. J. Bot. 30, 165–178
32 Hoch, G. and Martin, I. (1963) Arch. Biochem. Biophys. 102, 430–438
33 Rabinowitch, E.I. (1951) Photosynthesis, Vol. II, Part I, p. 685, Interscience Publishers, Inc., New York
34 Myers, J. (1971) Annu. Rev. Plant Physiol. 22, 289–312
35 Myers, J. and Graham, J.R. (1963) Plant Physiol. 38, 105–116
36 Joliot, P. (1965) Biochim. Biophys. Acta 102, 116–134
37 Thornber, J.P. and Highkin, H.R. (1974) Eur. J. Biochem. 41, 109–116
38 Haworth, P., Kyle, D.J. and C.J. Arntzen (1982) Arch. Biochem. Biophys. 218, 199–206
39 Punnett, T. (1971) Science 171, 284–286
40 Andersson, B. (1978) Ph.D. Thesis, Lund University, Sweden
41 Andersson, B. and Anderson, J.M. (1980) Biochim. Biophys. Acta 593, 426–436

42 Barber, J. (1982) Annu. Rev. Plant. Physiol. 33, 261–295
43 Kyle, D.J., Stahelin, L.A. and Arntzen, C.J. (1983) Arch. Biochem. Biophys. 222, 527–541
44 Andersson, B., Akerlund, H.E., Jergil, B. and Larsson, C. (1982) FEBS Lett. 149, 181–185
45 Schuster, G., Owens, G.C., Cohen, Y. and Ohad, I. (1983) in Abstr. 6th Int. Cong. Photosyn., p. 372, Brussels
46 Holmes, M.G. (1981) in Plants and the Daylight Spectrum (Smith, H., ed.), pp. 147–158, Academic Press, London
47 Telfer, A., Allen, J.F., Barber, J. and Bennett, J. (1983) Biochim. Biophys. Acta 722, 176–181